

# Two-step sintering and related properties of 10 vol.% ZrO<sub>2</sub>-Al<sub>2</sub>O<sub>3</sub> composites derived from filter and cold isostatic pressing

BARTOSZ WÓJTOWICZ\*, WALDEMAR PYDA

AGH-University of Science and Technology, Faculty of Materials Science and Ceramics, al. Mickiewicza 30, 30-059 Kraków  
\*e-mail: bartosz.wojtowicz@agh.edu.pl

## Abstract

This work presents a preparation of 10 vol.% zirconia-alumina composites with micrometer alumina and submicrometer zirconia grains via filter pressing and cold isostatic pressing for low temperature consolidation, and constant heating rate sintering (CHR), two-step sintering (TSS) and reverse two-step sintering (RTSS) for high temperature consolidation. The powders of nano-zirconia (10 nm) and alumina (175 nm) were used. Temperatures  $T_1$  and  $T_2$  of 1600°C and 1350°C were set for TSS, respectively. A reversed sequence of these temperatures was used for RTSS. The resultant composites were characterized in terms of density, microstructural features, hardness and fracture toughness. Both the forming method and the heating schedule showed negligible effects on density of the composites that were sintered using the heating schedules involving a temperature of 1600°C. The microstructure of composites was affected mainly by the heating schedule applied. The composite containing alumina grains of ~2.2 µm and uniformly dispersed zirconia grains of ~0.25 µm was obtained in case of the TSS schedule. The reversed two-step sintering (RTSS) delivered the most coarse-grained microstructures. The temperature  $T_1$  of 1600°C generated large grain growth ratios (10.8-18.5), resulting in the composites showing densities close to 95, but reasonably good hardness (20.8 ± 0.2 GPa) and fracture toughness (7.0 ± 0.2 MPa·m<sup>0.5</sup>).

**Keywords:** ZTA, Two step sintering, Microstructure - final, Mechanical properties, Composite

## DWUETAPOWE SPIEKANIE I ODPOWIEDNIE WŁAŚCIWOŚCI KOMPOZYTU 10 % obj. ZrO<sub>2</sub>-Al<sub>2</sub>O<sub>3</sub> WYTWORZONEGO DROGĄ PRASOWANIA FILTRACYJNEGO I IZOSTATYCZNEGO NA ZIMNO

W pracy przedstawiono wytwarzanie kompozytów 10 % obj. ZrO<sub>2</sub>-Al<sub>2</sub>O<sub>3</sub>, zawierających mikronowe ziarna tlenku glinu i submikronowe tlenku cyrkonu, za pomocą prasowania filtracyjnego i izostaticznego na zimno, w przypadku konsolidacji niskotemperaturowej, oraz spiekania ze stałą szybkością ogrzewania (CHR), spiekania dwuetapowego (TSS) i odwróconego spiekania dwuetapowego (RTSS), w przypadku konsolidacji wysokotemperaturowej. Wykorzystano proszki nanometrycznego ZrO<sub>2</sub> (10 nm) i Al<sub>2</sub>O<sub>3</sub> (175 nm). Dla schematu TSS ustalono temperatury  $T_1$  i  $T_2$  wynoszące odpowiednio 1600°C and 1350°C. Odwróconą sekwencję tych temperatur wykorzystano w przypadku schematu RTSS. Otrzymane kompozyty scharakteryzowano w kategoriach gęstości, cech mikrostrukturalnych, twardości i odporności na pękanie. Zarówno metoda formowania, jak i schemat ogrzewania miały zaniedbywalny wpływ na zagęszczenie kompozytów, które spieczono wykorzystując temperaturę 1600°C w schemacie ogrzewania. Na mikrostrukturę kompozytów główny wpływ miał schemat ogrzewania. Za pomocą schematu TSS otrzymano kompozyt zawierający ziarna tlenku glinu o rozmiarze ~2,2 µm i jednorodnie rozproszone ziarna tlenku cyrkonu o rozmiarze ~0,25 µm. Mikrostruktury pochodzące z odwróconego spiekania dwuetapowego (RTSS) były najbardziej gruboziarniste. Temperatura  $T_1$  wynosząca 1600°C spowodowała pojawienie się dużych współczynników rozrostu ziaren (10,8-18,5), które były przyczyną otrzymania kompozytów o gęstości wynoszącej blisko 95 %, ale wykazujących rozsądnie dobrą twardość (20,8 ± 0,2 GPa) i odporność na pękanie (7,0 ± 0,2 MPa·m<sup>0,5</sup>).

**Słowa kluczowe:** ZTA, spiekanie dwuetapowe, mikrostruktura, właściwości mechaniczne, kompozyt

## 1. Introduction

Two step sintering (TSS) is a simple, knowledge-based approach to powder consolidation, and has been developed by Chen and Wang [1]. In the first stage of sintering, the low temperature consolidated green sample is heated continuously to a temperature  $T_1$ , obtaining a density point of 75 % of theoretical density or more [2]. Then, the sample is cooled rapidly to a temperature  $T_2$ , and held for a long time (from a few to over a dozen hours), which is enough to yield full densification. In such a case, the advantageous difference in kinetics between grain boundary diffusion and

grain-boundary migration is generated, which suppresses the final-stage grain growth. The resultant material shows an optimized combination of the fine-grained, even nano-grained microstructure and high density, leading to improved any property which is small grain-size dependent.

The TSS method gives good results for both oxide and non-oxide one phase ceramics [3-12]. The reported mean grain sizes were a few times smaller than the size obtained for continuous rate sintering at the first stage temperature of TSS. Tartaj [10] has used a different schedule of two-step sintering with success for manufacturing crack free and dense monoclinic zirconia monoliths. The schedule of

low-high temperatures was applied due to the temperature limit imposed by the m-t transformation in pure ZrO<sub>2</sub>. The approach utilized benefits of low-temperature sintering.

There has been only few attempts of two-step sintering in case of the composite materials. Ye *et al.* [13] used the two-step sintering in processing silicon nitride-barium aluminosilicate composite material. As a result of TSS, the modified microstructure evolution, bending strength and fracture toughness have been increased, but hardness of the TSS samples appeared lower than in the case of natural sintering. Wang *et al.* [14] manufactured high-density alumina-5 wt % zirconia ceramics using the two-step method. A composite with small grain size in the range of 0.62-0.88 μm and density close to theoretical one (over 99 %) was obtained; neither hardness nor fracture toughness were examined.

In this paper, two-step-sintering of 10 vol.% nano-zirconia-alumina composite powder processed by filter and cold isostatic pressing is described. Two schedules of heating temperatures were applied: high-low and low-high, and compared with the constant heating rate schedule. Effects of compaction method and sintering schedule on microstructure evolution and some mechanical properties of the zirconia-alumina composite are studied.

## 2. Experimental

Zirconia nano-powder of a mean particle size of 35 nm and isometric crystallite shape was obtained by hydrothermal crystallization of precipitated hydrous zirconia gel under ~3 MPa for 8 h at 240°C in the environment of 2 M NaCl solution. Zirconium oxychloride (purity > 99 %, Si - 0.03 %, Fe - 0.02 %, Al - 0.015 %) and aqueous ammonia (analytically pure) were used for precipitation of the gel. High-purity alumina AKP-30 powder with no sintering additives from Sumitomo Chemical Co. was used in the study.

A mixture of component powders composed of 90 vol.% AKP-30 and 10 vol.% zirconia (called as ZTA) was prepared by attrition milling in water acidulated to pH of 2.5. Just before the end of the milling, the pH value was increased up to 9 by using aqueous ammonia to induce a heteroflocculation effect. Then, one part of the slurry was dried at 105°C, and the resultant powder was pressed uniaxially under 50 MPa with the addition of 3 wt % mineral oil based lubricant first, and then cold isostatically under 300 MPa (CIP). The rest of the flocked slurry was filter pressed under 5.5 MPa (FP). The wet green compacts were dried to constant weight in the presence of silica gel in a desiccator. The pure alumina powder compacts were also prepared by using the above mentioned procedures of filter and cold isostatic pressing. The green ZTA compacts derived from the FP and CIP methods were sintered using the following temperature schedules: (i) 1350°C for 8 h, (ii) 1600°C for 2 h, (iii) 1600°C for 0 h followed by 1350°C for 8 h, and (iv) 1350°C for 8 h followed by 1600°C for 2 h. A heating rate of 10°C/min and furnace cooling were applied between the soaking steps. The sintering schedules (i) and (ii) represent normal constant heating rate sintering (CHR); the schedule (iii) refers to the two-stage sintering reported by Chen *et al.* [1] for nanocrystalline Y<sub>2</sub>O<sub>3</sub> ceramics (TSS), and the schedule (iv) follows the Tartaj's approach [10] (reversed two-stage sintering – RTSS) applied for sintering nanosize pure zirconia. The sintering was

preceded by dilatometry measurements to determine the sintering  $T_1$  and  $T_2$  temperatures for the two-step sintering. The measurements were performed in air using a DIL 402C (Netzsch) apparatus and a heating rate of 10°C/min.

The AKP-30 and nano-zirconia powders were characterized by using electron transmission microscopy (JEM-1011, Jeol) and BET method (Nova 1200e, Quantachrome Inc).

The pore size distribution was measured by mercury porosimetry using a Quantachrome PoreMaster 60 apparatus. The density of sintered bodies was determined by Archimedes method. The microstructure of the samples was examined by SEM (FEI Nova 200 NanoSEM). The grain size was obtained by multiplying by 1.56 the average linear intercept length of at least 100 grains.

Both Vickers hardness and fracture toughness measurements were performed using a FV-700 Vickers Hardness Test apparatus. A load of 9.81 N and 98.1 N was applied, respectively. The Palmqvist crack model was used for fracture toughness calculations [15].

## 3. Results and discussion

### 3.1. Powders and green compacts

TEM images of the zirconia and alumina powders are shown on Fig. 1. The AKP-30 powder has the particle size of 0.3-0.5 μm and BET surface area of 8.6 m<sup>2</sup>/g with equivalent particle size  $d_{BET} = 175$  nm. The zirconia powder has the mean grain size of ~10 nm and surface area of 80 m<sup>2</sup>/g.

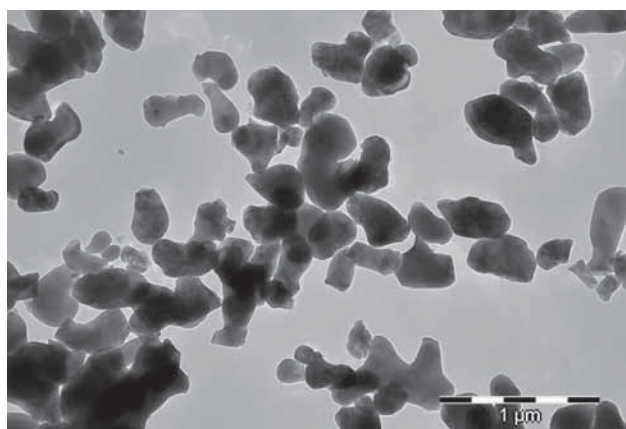
Table 1. Density of green samples.  
Tabela 1. Gęstość surowych próbek.

Sample	Filter pressing		Cold isostatic pressing	
	AKP	ZTA	AKP	ZTA
Density [%]	52.4 ± 0.5	49.9 ± 0.3	58.4 ± 0.3	55.5 ± 0.6

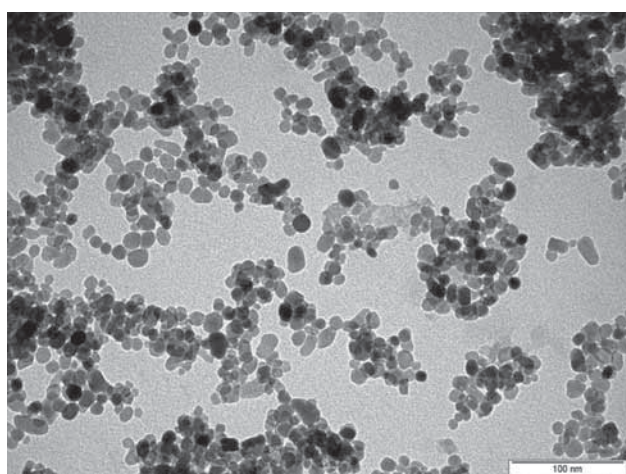
The densities of green samples are shown in Table 1. It can be seen that the cold isostatically pressed samples have higher density than filter pressed by 5.6-6 %. The addition of zirconia nano-powder made more difficult particle packing within compacts during pressing, and total porosity of the ZTA samples was smaller than originated from the AKP-30 (AKP). However, pore sizes shifted towards smaller values due to incorporation of the nanometric zirconia crystallites into the space among bigger alumina particles, as indicated by the pore size distribution curves shown in Fig. 2.

### 3.2 Determination of sintering temperatures

The results of two-step sintering strongly depend on the choices of temperature  $T_1$  and  $T_2$  [1]. Constant rate heating of a sample to the higher temperature  $T_1$  must yield a density higher than 75 % and a state in which all pores in the microstructure are still unstable and can shrink. In this study,  $T_1$  has been chosen taking into consideration both literature data [14] and the evolution of densification rate ( $d\rho/dt$ ) derived from a DIL experiment. The data shown in Fig. 3 indicate that a maximum of densification rate was not attained within the temperature range applied. So, the final



a)



b)

Fig. 1. TEM images of the powders used: a) AKP-30, b) hydrothermal nano-zirconia.

Rys. 1. Obrazy TEM użytych próbek: a) AKP-30, b) hydrotermalny nano-ZrO<sub>2</sub>.

sintering stage attributed to the exhausting of densification rate [16] is not observed and only the arbitrary temperature  $T_1$  can be indicated. The densification rate curve in Fig. 3 is shifted  $\sim 50^\circ\text{C}$  towards higher temperatures when compared to the data reported by Wang *et al.* [14], suggesting the corresponding shift of the appropriate  $T_1$  temperature range for the studied zirconia-alumina system. Simple linear approximation of the data shown in Fig. 3 indicates the temperature of  $1500^\circ\text{C}$  being suitable for obtaining the relative density of 75 %. Taking above into consideration and accepting a risk originating from over-heating and corresponding grain growth, a temperature of  $1600^\circ\text{C}$  was selected for the first step of sintering.

The temperature of the second step of sintering is also very important because too low  $T_2$  can exhaust the densification due to the suppression of atomic diffusion, but too high  $T_2$  can generate the grain growth. For the second step of sintering, the temperature  $T_2$  was set at  $1350^\circ\text{C}$ , critically analyzing previous research reports [1, 8, 12, 14].

### 3.3. Characterization of sinters

The densification data of the filter or cold isostatic pressed ZTA composites followed by high temperature consolidation using the CHR, TSS and RTSS schedules are shown

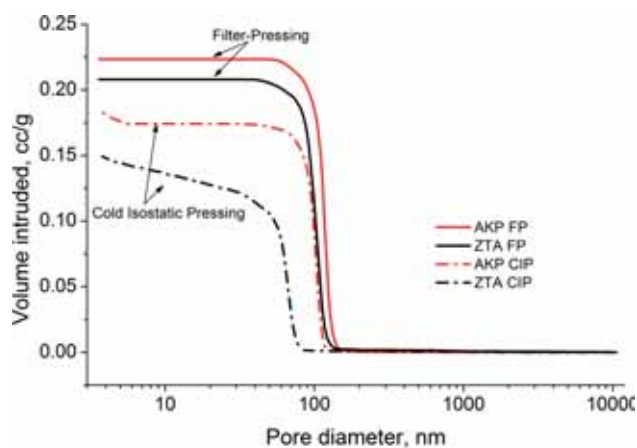


Fig. 2. Cumulative curves of pore size distribution of composite (ZTA) and alumina powder (AKP) compacts filter (FP) and cold isostatic (CIP) pressed.

Rys. 2. Krzywe kumulacyjne rozkładu wielkości porów wyprasek z proszków kompozytowego (ZTA) i tlenku glinu (AKP) prasowanych filtracyjnie (FP) i izostatycznie na zimno (CIP).

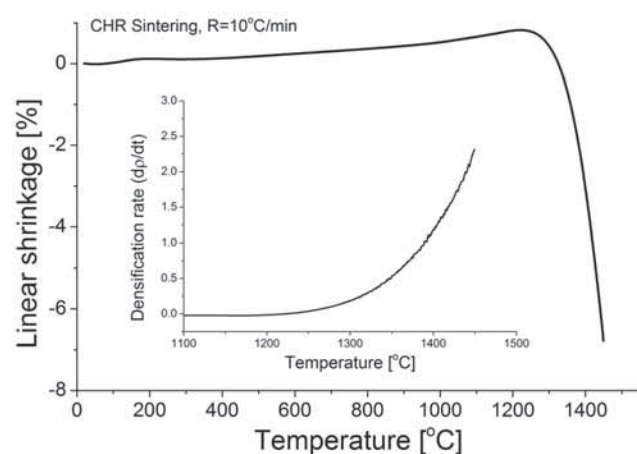


Fig. 3. Dilatometric curve of ZTA composite powder filter pressed under  $5.5\text{ MPa}$ . An inset shows densification rate as a function of temperature for constant-rate (CHR) sintering.

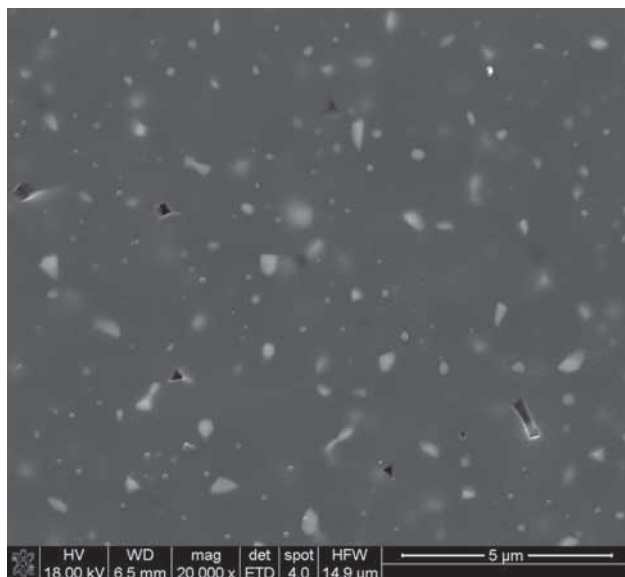
Rys. 3. Krzywa dylatometryczna proszku kompozytowego ZTA prasowanego filtracyjnie pod ciśnieniem  $5.5\text{ MPa}$ . Wkładka pokazuje zależność szybkości zagęszczania w funkcji temperatury w przypadku spiekania przy stałej szybkości ogrzewania (CHR).

in Table 2. The effect of the powder forming method on the composite density is detectable only at the lowest sintering temperature applied (CHR<sub>1</sub>). Filter pressing resulted in less dense sintered samples ( $\sim 5\%$ ) than cold isostatic pressing due to  $\sim 6\%$  lower green density of the FP compacts. The composite density was not affected by powder forming method at higher temperature of natural sintering (CHR<sub>2</sub>) and during the two-step sintering schedules (TSS and RTSS). The difference in density among the compacts sintered by using the CHR<sub>2</sub>, TSS and RTSS schedules is insignificant, and the values of density close to 95 % are moderate. This suggests that the temperature  $T_1$  was set to high, and kinetics of grain boundary migration exceeded kinetics of grain boundary diffusion, generating the excessive grain growth, leading to a stable state of pores and, as a result, the large amount of porosity.

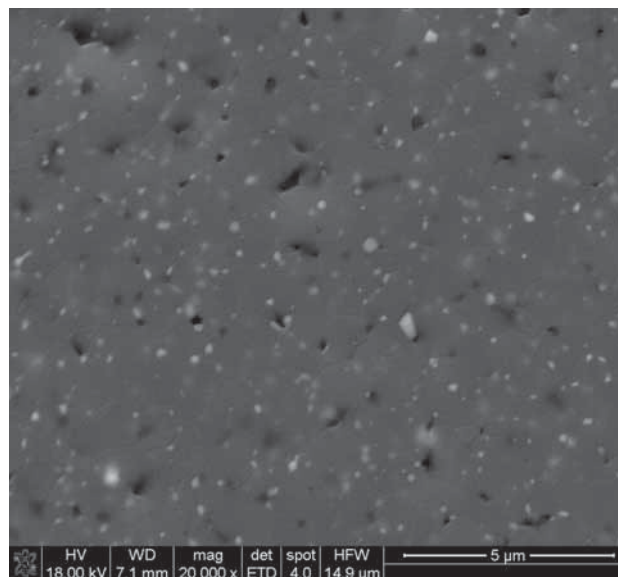
The above conclusion is confirmed by microstructural observations. The results shown in Figs. 4-6 and in Table 2

Table 2. Relative density and grain size of the sintered ZTA samples.  
Tabela 2. Gęstość względna i rozmiar ziaren spieczonych próbek ZTA.

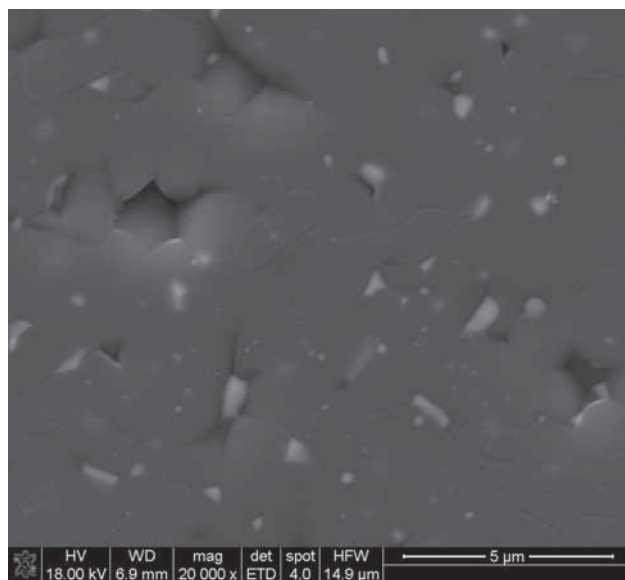
Schedule	Sintering conditions	Relative density [%]		Grain size [ $\mu\text{m}$ ]	
		FP	CIP	FP	CIP
CHR <sub>1</sub>	1350°C/8h	71.57 $\pm$ 0.30	78.12 $\pm$ 0.21	-	-
CHR <sub>2</sub>	1600°C/2h	95.80 $\pm$ 0.52	94.83 $\pm$ 0.08	3.0	2.9
TSS	1600°C/0h+1350°C/8h	94.29 $\pm$ 0.34	94.56 $\pm$ 0.31	2.1	2.2
RTSS	1350°C/8h+1600°C/2h	94.37 $\pm$ 0.16	94.32 $\pm$ 0.33	3.4	4.0



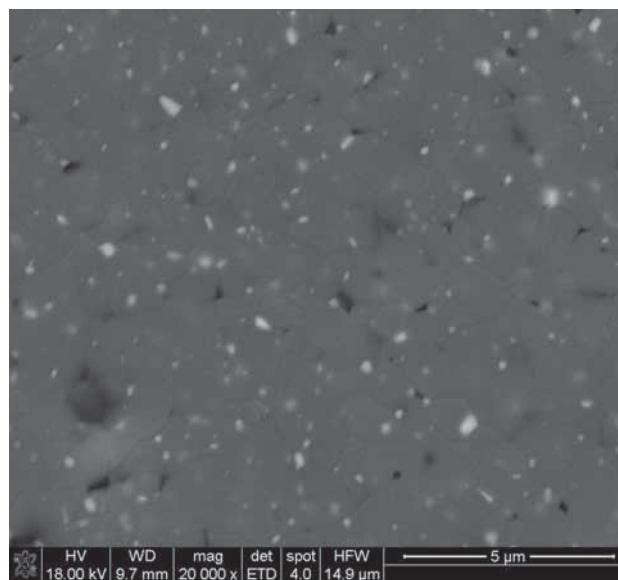
a)



a)



b)



b)

Fig. 4. SEM images of the microstructure of the ZTA compacts sintered for 8 h at 1350°C and additionally for 2 h at 1600°C: a) filter pressed compact, b) cold isostatic pressed compact.

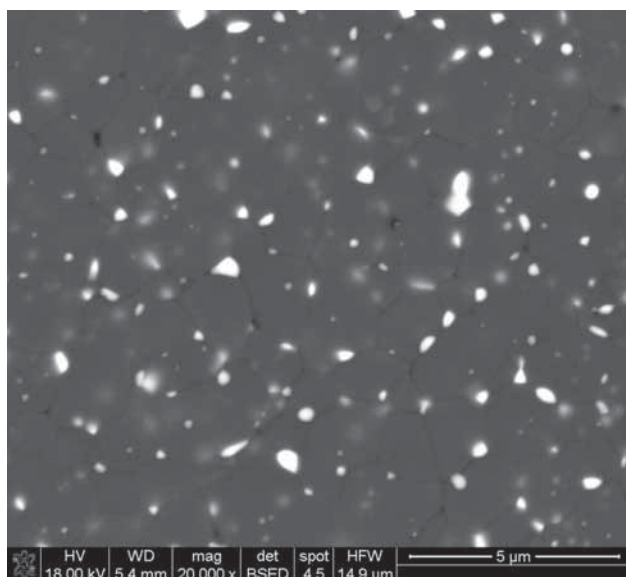
Rys. 4. Obrazy SEM mikrostruktury wyprasek ZTA spieczonych przez 8 h w 1350°C i dodatkowo przez 2 h w 1600°C: a) wypraska prasowana filtracyjnie, b) wypraska prasowana izostatycznie na zimno.

indicate large alumina grain sizes practically aside from the forming method applied for low temperature consolidation of the composite powder. The grain growth ratio (final grain size/initial particle size – 0.2  $\mu\text{m}$ ; calculated as an average

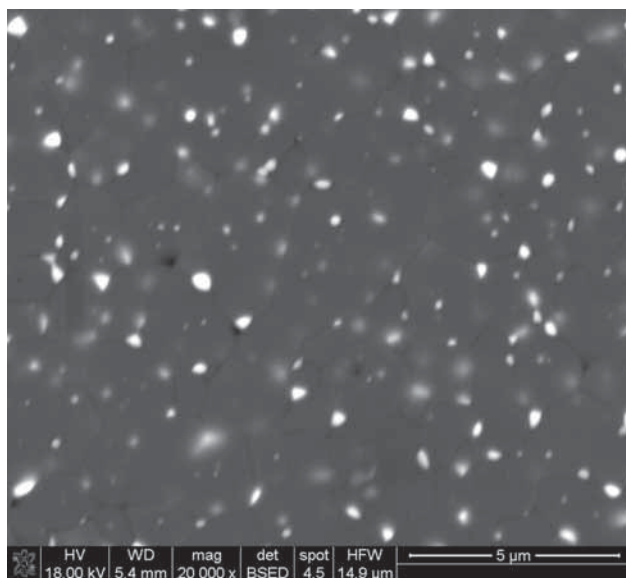
Fig. 5. SEM images of the microstructure of the ZTA compacts sintered for 0 h at 1600°C and additionally for 8 h at 1350°C: a) filter pressed compact, b) cold isostatic pressed compact.

Rys. 5. Obrazy SEM mikrostruktury wyprasek ZTA spieczonych przez 0 h w 1600°C i dodatkowo przez 8 h w 1350°C: a) wypraska prasowana filtracyjnie, b) wypraska prasowana izostatycznie na zimno.

for FP and CIP) is 14.8, 10.8 and 18.5, for the CHR<sub>2</sub>, TSS and RTSS schedules, respectively. The advantageous microstructural result is observed for TSS when compared to other heating schedules; the microstructure composed



a)



b)

Fig. 6. SEM images of the microstructures of the samples sintered at 1600°C for 2 h: a) filter pressing and b) cold isostatic pressing.  
Rys. 6. Obrazy SEM mikrostruktur próbek spieczonych w 1600°C przez 2 h: a) prasowanie filtracyjne, b) prasowanie izostacyjne na zimno.

of alumina grains of  $\sim 2.2 \mu\text{m}$  and uniformly dispersed zirconia grains of  $\sim 0.25 \mu\text{m}$  was obtained (Fig. 5). Two-step sintering in the reversed temperature mode gave the most coarse-grained microstructures, concerning both alumina and zirconia grains:  $3.7 \mu\text{m}$  and  $0.54 \mu\text{m}$ , respectively. The  $\text{CHR}_2$  schedule led to the alumina and zirconia grain sizes of  $3.0 \mu\text{m}$  and  $0.39 \mu\text{m}$ , respectively.

Table 3. Vickers hardness,  $H_v$ , and fracture toughness,  $K_{Ic}$ , of the ZTA samples.  
Tabela 3. Twardość Vickersa,  $H_v$ , i odporność na pękanie,  $K_{Ic}$ , próbek ZTA.

Schedule	Sintering conditions	Forming method	$H_v$ [GPa]	$K_{Ic}$ [ $\text{MPa}\cdot\text{m}^{0.5}$ ]
$\text{CHR}_2$	1600°C/2h	CIP	$17.02 \pm 0.24$	$5.93 \pm 0.28$
TSS	1600°C/0h+1350°C/8h	FP	$20.83 \pm 0.22$	$7.02 \pm 0.12$
		CIP	$19.36 \pm 0.29$	$5.61 \pm 0.33$
RTSS	1350°C/8h+1600°C/2h	FP	$18.96 \pm 0.36$	$6.26 \pm 0.16$
		CIP	$17.81 \pm 0.31$	$6.21 \pm 0.15$

The SEM pictures (Figs. 4-6) show that zirconia grains are uniformly dispersed in the alumina matrix. The zirconia particles are located mainly in grain boundaries or triple junctions of alumina. This proves the presence of the pinning effect, generating inhibition of the alumina grain growth. However, some zirconia particles form intra-grain inclusions, indicating very fast kinetics of grain-boundary migration at the temperature  $T_1$  applied.

The results of Vickers hardness and fracture toughness tests are shown in Table 3. The influence of both the powder forming method and heating schedule on the mechanical properties can be clearly seen, as a result of the previously characterised features of the composite microstructures, and most probably the features that were not studied in this work, e.g. a pore size and a pore size distribution. This concerns especially origins of the difference in mechanical properties between the materials derived from filter and cold isostatic pressing. The filter pressed sample sintered by using the TSS schedule shows the largest values of both hardness and fracture toughness. Slightly lower values were obtained in the case of the CIP/TSS composite, which also showed the similar fine grained microstructure (Fig. 5). It is worthy to remark that the reasonably good mechanical properties were obtained in case of the not fully densified materials.

#### 4. Conclusions

The alumina matrix composites containing 10 vol.% zirconia were manufactured by using filter pressing (FP) and cold isostatic pressing (CIP) for low temperature consolidation, and constant heating rate sintering (CHR), two-step sintering (TSS) and reverse two-step sintering (RTSS) for high temperature consolidation. The powders of nano-zirconia (10 nm) and alumina (175 nm) were used

There were negligible effects of both the forming method and the heating schedule on densification of the composites sintered using the heating schedules involving a temperature of 1600°C, which was selected as the temperature of the first step of sintering.

The microstructure of composites was affected mainly by the heating schedule applied. The composite containing alumina grains of  $\sim 2.2 \mu\text{m}$  and uniformly dispersed zirconia grains of  $\sim 0.25 \mu\text{m}$  was obtained in case of the TSS schedule. The reversed two-step sintering (RTSS) led to the most coarse-grained microstructures, and is not recommended for densification of ZTA composites using the studied heating schedule.

The temperature  $T_1$  of 1600°C generated large grain growth ratios (10.8-18.5), resulting in the composites showing densities close to 95 %, but reasonably good hardness ( $20.8 \pm 0.2 \text{ GPa}$ ) and fracture toughness ( $7.0 \pm 0.2 \text{ MPa}\cdot\text{m}^{0.5}$ ).

Temperature  $T_1$  for the first step of sintering should be set below 1600°C.

## Acknowledgements

The work was financially supported by the European Union within a framework of European Regional Development Found under Innovative Economy Operating Programme; grant no. POIG.01.03.01-00-024/08. The authors would like to thank Mrs. B. Trybalska, dr. P. Rutkowski and Mr. R. Lach for their assistance in SEM, DIL and BET/porosimetry measurements, respectively.

## References

- [1] Chen I.W., Wang X.H.: „Sintering dense nanocrystalline ceramics without final-stage grain growth”, *Nature*, 404, (2000), 168-171.
- [2] Maca K., Pouchly V., Zalud P.: „Two-Step Sintering of oxide ceramics with various crystal structures”, *J. Eur. Ceram. Soc.*, 30, (2010), 583-589.
- [3] Durán P., Capel F., Tartaj J., Moure C.: „A strategic two-stage low-temperature thermal processing leading to fully dense and fine-grained doped-ZnO varistors”, *Adv. Mater.*, 14, 2, (2002), 137-141.
- [4] Polotai A., Breece K., Dickey E., Randall C., Ragulya A.: „A novel approach to sintering nanocrystalline barium titanate ceramics”, *J. Am. Ceram. Soc.*, 88, 11, (2005), 3008-3012.
- [5] Wang X.H., Deng X.Y., Bai H.L., Zhou H., Qu W.G., Li L.T., Chen I.W.: „Two-step sintering of ceramics with constant grain-size. II. BaTiO<sub>3</sub> and Ni-Cu-Zn ferrite”, *J. Am. Ceram. Soc.*, 89, 2, (2006), 438-443.
- [6] Yu P.C., Li Q.F., Fuh J.Y.H., Li T., Lu L.: „Two-stage sintering of nanosized yttria stabilized zirconia processed by powder injection moulding”, *J. Mater. Process. Tech.*, 192-193, (2007), 312-318.
- [7] Binner J., Annapoorani K., Paul A., Santacruz I., Vaidhyanathan B.: „Dense nanocrystalline zirconia by two stage conventional/hybrid microwave sintering”, *J. Eur. Ceram. Soc.*, 28, 5, (2007), 973-977.
- [8] Bodišová K., Šajgalík P., Galusek D., Švancárek P.: „Two-stage sintering of alumina with submicrometer grain size”, *J. Am. Ceram. Soc.*, 90, 1, (2007), 330-332.
- [9] Lee Y.I., Kim Y.W., Mitomo M.: „Effect of processing on densification of nanostructured SiC ceramics fabricated by two-step sintering”, *J. Mater. Sci.*, 39, (2004), 3801-3803.
- [10] Tartaj J.: „Two-Stage Sintering of Nanosize Pure Zirconia”, *J. Am. Ceram. Soc.*, 92, S1, (2009), S103-S106.
- [11] Mazaheri M.: „Sintering of Nanocrystalline Zinc Oxide via Conventional Sintering, Two Step Sintering and Hot Pressing”, *Materiały Ceramiczne/Ceramic Materials*, 62, 4, (2010), 506-509.
- [12] Ragulya A.V.: „Consolidation of ceramic nanopowders”, *Advances in Applied Ceramics*, 107, 3, (2008), 118-134.
- [13] Ye F., Liu L., Zhang J., Iwasa M., Su C.L.: „Synthesis of silicon nitride-barium aluminosilicate self-reinforced ceramic composite by a two-step pressureless sintering”, *Comp. Sci. Tech.*, 65 (2005), 2233-2239.
- [14] Wang Ch.J., Huang Ch.Y., Wu Y.Ch.: „Two step sintering of fine alumina-zirconia ceramics”, *Ceram. Int.*, 35, 4, (2009), 1467-1472.
- [15] Niihara K.: „A fracture mechanics analysis of indentation-induced Palmqvist cracks in ceramics”, *J. Mater. Lett.*, 2, (1983), 221.
- [16] Hansen J.D., Rusin R.P., Teng M.H., Johnson D.L.: „Combined stage sintering model”, *J. Am. Ceram. Soc.*, 75, 5, (1992), 1129-1135.

◆

Otrzymano 3 listopada 2011; zaakceptowano 9 grudnia 2011